Extended Abstracts of the 22nd (1990 International) Conference on Solid State Devices and Materials, Sendai, 1990, pp. 425-428

A New Mechanism of Failure in Silicon p^+/n Junction Induced by Diffusion Barrier Metals

Y. Igarashi, T. Yamaji and S. Nishikawa

Semiconductor Technology Laboratory, OKI Electric Industry Co., Ltd.
550-5 Higashiasakawa-cho, Hachioji-shi, Tokyo 193, Japan

The mechanism of failure of p^+/n and n^+/p junctions under Al-Si/TiN/Ti and Al-Si/ZrN/Zr systems at contact holes has been investigated. When a total force of the barrier metal in the metallization system, which is defined as the sum of products of each film stress and film thickness, is larger than $3x10^5$ dyn/cm, the junction leakage current increases on p^+/n diodes, but not on n^+/p diodes after annealing at 500°C. This increase is caused by the formation of dislocation loop in p^+-Si. The formation depends on the annealing temperature, the total force of barrier metal and the B concentration. On the B concentration of $2x10^{20}/cm^3$ and the total force of more than $3x10^5$dyn/cm, the dislocations are generated after even 400°C annealing. The shear stress resolved on the slip plane in the slip direction concentrates at the contact hole edge, which is consistent with the result of TEM observation.

1.INTRODUCTION Mechanical stress in interconnection structures has long been a problem in VLSI devices, and the introduction of new materials and processes is increasing the severity of the problem. Refractory metal nitrides, such as TiN and ZrN, have been investigated as diffusion barriers between aluminum films and silicon substrates[1,2]. These materials have high compressive stress as large as several 10^{10}dyn/cm^2. When the stress exceeds the strength of the films or that of the adhesion to substrates, crack and delamination, which are the main failure modes of these films, occur[3]. Junction leakage caused by generation of micro cracks in the barrier metal has been reported[3,4]. In this report, we have investigated the characteristics of contacts between Al-Si lines with ZrN or TiN as barrier metals and p^+- or n^+-Si layers, and found a new failure mode of junction leakage induced by the large stress of TiN and ZrN.

2.EXPERIMENTAL p^+/n and n^+/p diodes with parameters shown in Table 1 were formed by a typical CMOS process. Two types of metallization structure, Al-1%Si(4000Å)/ZrN/Zr(100Å) and Al-1%Si(4000Å) /TiN/Ti(100Å), were used. ZrN and TiN films, which were prepared by N_2 reactive sputtering with a bias voltage, had mechanical stresses of $-2.5x10^{10}$ and $-4x10^{10}$dyn/cm^2 in the compressive direction, respectively. After the metallization, these samples were annealed at temperatures in the range of 400-500°C for 1 hour. Junction leakage current was measured after annealing.

3.RESULTS AND DISCUSSION

3.1. Junction leakage by dislocation formation

As shown in Fig.1, the reverse currents of p^+/n diodes with 1200Å-thick ZrN and all n^+/p diodes after 500°C annealing are as small as those with the conventional Al-Si/Si contacts after 400°C annealing, but those of the p^+/n diodes with 2200Å-thick ZrN and 1500Å-thick TiN are unacceptably high. These facts indicate that a leakage path, which may be current-generating defects

Table 1 Parameters of diffusion layers. (simulated)

	p^+-contact	n^+-contact	
Dopant (Implant ion)	B (BF_2^+)	As (As^+)	& P (P^+)
Surface dopant concentration(/cm^3)	$2x10^{20}$	$7x10^{20}$	$3x10^{20}$
Surface carrier concentration(/cm^3)	$2x10^{20}$	$4x10^{20}$	
Junction depth(μm)	0.27	0.43	

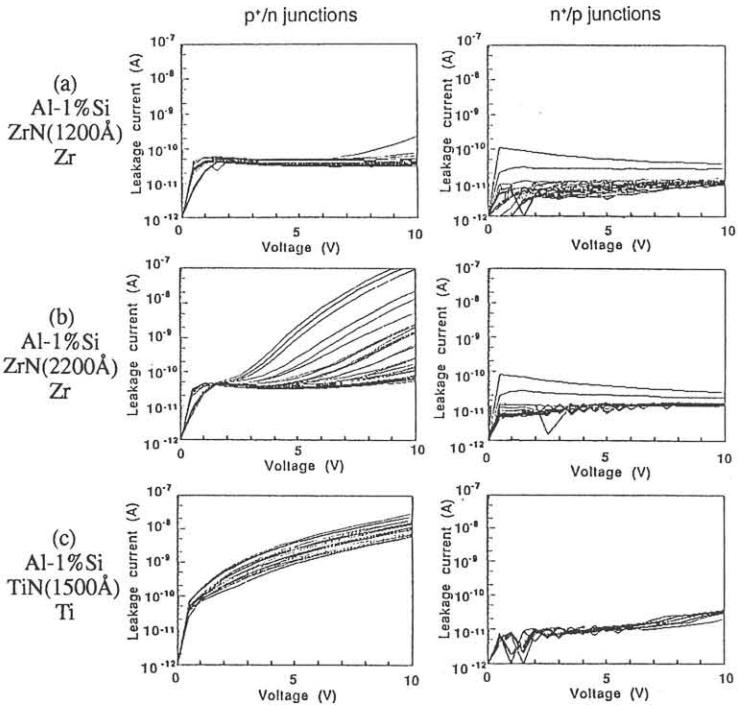

Fig.1 Leakage currents of p^+/n and n^+/p diodes annealed at 500°C after metallization.

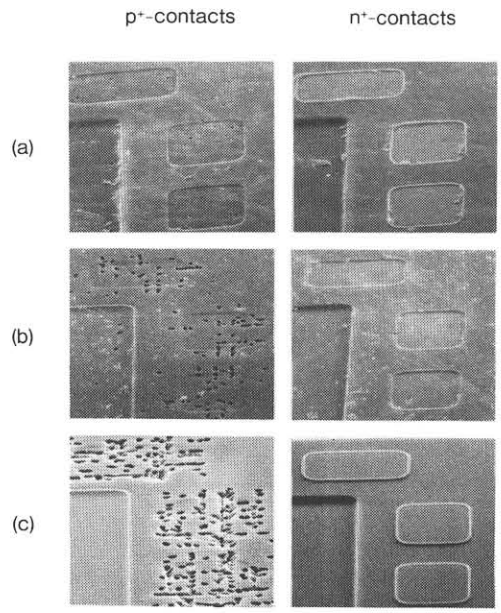

Fig.2 SEM photographs of contact areas of the samples in Fig.1 after Secco etching.

in the depletion layer, is newly formed by the annealing at 500°C. The defects are clearly revealed as etch pits in Fig.2. The etch pits induced by dislocation loops, which are confirmed by TEM observation as shown in Fig.3, are observed in high density on the p^+-contact regions giving high leakage current, but not on the n^+-contact regions. The shape of these dislocations in Fig.3 suggests that dislocation sources exist on the edges of contact holes.

3.2. Stress analysis The stress analysis of the contact region was performed by two dimensional finite-element simulation. To consider the shear stresses acting on the dislocation formation, computed stresses were resolved on {111} slip planes in <110> slip directions[5]. These planes and directions are illustrated through the elemental octahedron in Fig.4(a). This model has four independent slip directions. Taking account of the hypotheses of this simulation that a structure on the z-direction is infinite, the shear stresses in these directions are as follows:

$$S_{(\bar{1}11)\langle\bar{1}\bar{1}0\rangle} \equiv S0 = 0,$$

$$S_{(\bar{1}11)\langle 01\bar{1}\rangle} \equiv S1 = \sqrt{1/6}\,(\sigma_x - \sigma_y) - 1/2\cdot\sqrt{1/3}\,\sigma_{xy},$$

$$S_{(111)\langle 01\bar{1}\rangle} \equiv S1' = \sqrt{1/6}\,(\sigma_z - \sigma_y) + 1/2\cdot\sqrt{1/3}\,\sigma_{xy},$$

$$S_{(\bar{1}\bar{1}1)\langle 10\bar{1}\rangle} \equiv S2 = \sqrt{1/6}\,(\sigma_x - \sigma_y) + 1/2\cdot\sqrt{1/3}\,\sigma_{xy},$$

$$S_{(111)\langle 10\bar{1}\rangle} \equiv S2' = \sqrt{1/6}\,(\sigma_z - \sigma_y) - 1/2\cdot\sqrt{1/3}\,\sigma_{xy},$$

$$S_{(111)\langle\bar{1}10\rangle} \equiv S3 = \sqrt{1/3}\,\sigma_{xy},$$

where $S_{(abc)\langle abc\rangle}$ means the shear stress on the (abc) slip plane in the <abc> slip direction. Other directions are eliminated for the crystallographic symmetry. In this work, we estimated S0,S1,S2 and S3, because σ_z can not calculate on the two dimensional simulation. Figure 4(c) shows absolute stress profiles of the resolved directions, which are normalized by the maximum stress. In the vicinity of contact hole edge, the maximum stress generates in S3. Therefore, dislocations will be generated at contact hole edge by this shear stress, and glide on the slip plane including the direction of S3. The dislocations on this slip plane are observed in the TEM photograph shown in Fig.3.

3.3. Mechanism for the formation of dislocation

For p^+/n diodes the relationship between the leakage current and the etch pit density is shown in Fig.5 as a function of annealing temperature and total force of metallization layers which is defined as the sum

of products of each film stress and film thickness. The critical total force, when dislocations are formed, is about $3x10^5$ dyn/cm in the annealing temperature range of 400-500°C. At 400°C, dislocations are formed but no junction leakage is observed. This is consistent with an inference that the leakage starts only when dislocations cross the junction as discussed above. Figure 6 shows leakage characteristics of two diodes which are different in the surface concentration of B with the same junction depth and the same total force. The leakage originated by the dislocation formation increases with the surface concentration of B. The spreading resistance (SR) measurement and process simulation show that most of these B atoms are at substitutional sites. The substitutional B contracts Si lattice, because of small tetrahedral radius of B (0.88Å) in comparison with that of Si (1.77Å)[6]. According to Queisser's work[7], dislocations are generated by the lattice contraction in B diffusion layer, when B concentration and annealing temperature are more than $1x10^{20}/cm^3$ and 1000°C, respectively. His results show that the number of dislocation increases with the strain which is in proportional to the concentration of substitutional B. In our experiment, the annealing temperature of 400-500°C is much lower than that of Queisser's experiments. The external stress induced by the total force of barrier metal acts on Si lattice, besides the internal stress induced by substitutional B. The generation of dislocation is enhanced by the external stress, in cooperation with the internal stress. On n^+-contacts, the strain originated by substitutional As and P is small in comparison with the B case on p^+-contacts[6,8]. Therefore, the generation of dislocation is suppressed even on the same condition as p^+-contact.

Our present results show that in some cases the stress in Si induced by high stress of films deposited on it exceeds the strength of Si even in relatively low temperature processes. We must, therefore, precisely control the stress in Si induced by processes and materials to realize future ULSI's.

4.CONCLUSION The mechanism of failure of p^+/n and n^+/p junctions under Al-Si/TiN/Ti and Al-Si /ZrN/Zr systems at contact holes has been investigated.

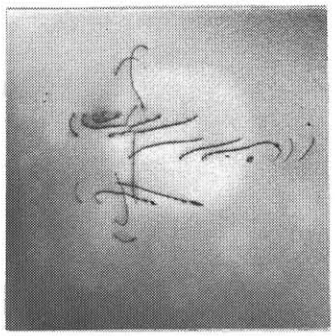

Fig.3 TEM photograph of p^+ contact area.

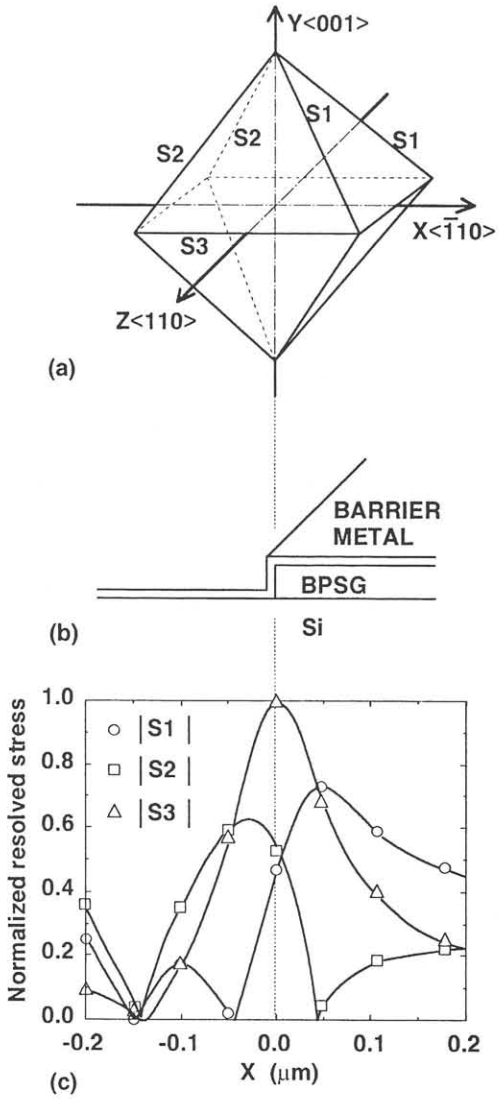

Fig.4 (a) Elemental octahedron showing slip planes and slip directions in single-crystal silicon; (b) Schematic diagram of a part of contact hole used in the simulation; (c) Distribution of the normalized stresses resolved on the three independent slip systems in the vicinity of contact hole edge.

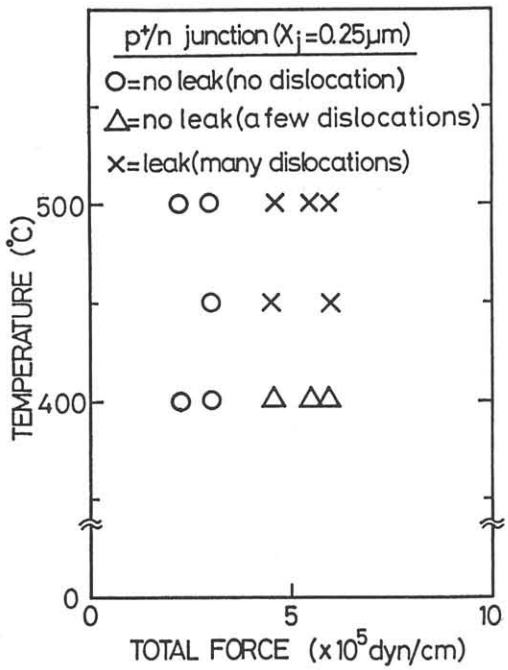

Fig.5 Dislocation generation and junction leak as a function of total force and annealing temperature.

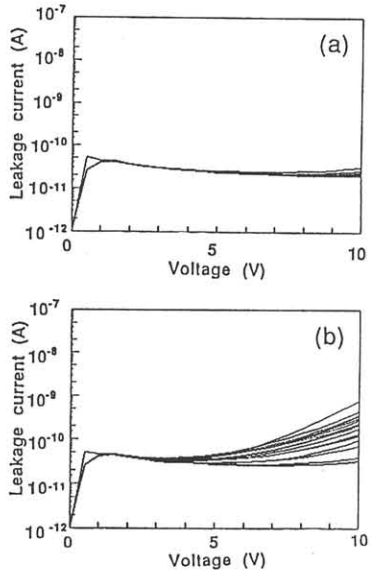

Fig.6 Dependence of surface concentration of B. (a): $0.8\times10^{20}/cm^3$; (b): $2\times10^{20}/cm^3$. (junction depth: about 0.25μm; total force: 3.0×10^5dyn/cm; annealing temperature: 500°C)

When the total force of barrier metal in the metallization system is larger than 3×10^5dyn/cm, the junction leakage current increases on p^+/n diodes, but not on n^+/p diodes after 500°C annealing. This increase is caused by the formation of dislocation loop in p^+-Si. The formation depends on the annealing temperature, the total force of the metallization layers and the surface concentration of B. The stress analysis using finite-element simulation shows that the shear stress concentrates at the contact hole edge. These findings suggest that the generation of dislocation is enhanced by the external stress induced by the total force of barrier metal, in cooperation with the internal stress induced by substitutional B.

ACKNOWLEDGMENTS

The authors are grateful to Dr. S.Ohono for helpful advice. They also thank Mr.Ochiai for useful advice in the electrical measurements.

REFERENCES

1) M.Wittmer; Appl. Phys. Lett. **37** (1980) 540
2) L.Krusin-Elbaum, M.Wittmer, C.-Y.Ting and J.J.Cuomo; Thin Solid Films **104** (1983) 81
3) A.Kohlhase, M.Mändl and W.Pamler; J. Appl. Phys. **65** (1989) 2464
4) N.Kumar, M.G.Fissel, K.Pourrezaei, B.Lee and E.C.Douglas; Thin Solid Films **153** (1987) 287
5) G.Bentini, L.Correra and C.Donolato; J. Apply. Phys. **56** (1984) 2922
6) K.G.Mcquhae and A.S.Brown; Solid-State Electron. **15** (1972) 259
7) H.J.Queisser; J. Appl. Phys. **32** (1961) 1776
8) C.K.Huang and R.J.Jaccodine; J. Appl. Phys. **66** (1989) 531